ACSNANO
www.acsnano.org
ARTICLE

Carbon Nanotube Macroelectronics for Active Matrix Polymer-Dispersed Liquid Crystal Displays

Sen Cong,[†] Yu Cao,[†] Xin Fang,[§] Yufeng Wang,[†] Qingzhou Liu,[§] Hui Gui,[§] Chenfei Shen,[§] Xuan Cao,[§] Eun Sok Kim,[†] and Chongwu Zhou*[,†]

[†]Ming Hsieh Department of Electrical Engineering and [§]Mork Family Department of Chemical Engineering and Materials Science, University of Southern California, Los Angeles, California 90089, United States

Supporting Information

ABSTRACT: **Active matrix liquid crystal display (AMLCD) is the most widely used display technology nowadays. Transparent display is one of the emerging technologies to provide people with more features such as displaying images on transparent substrates and simultaneously enabling people to see the scenery behind the panel. Polymer-dispersed liquid crystal (PDLC) is a possible active matrix transparent display technology due to its high transparency, good visibility, and low power consumption. Carbon nanotubes (CNTs) with excellent mobility, high transparency, and room-temperature processing compatibility are ideal materials for the driver circuit of the PDLC display. Here, we report the monolithic integration of CNT thin-film transistor driver circuit with PDLC pixels. We studied the transmission properties of the PDLC pixels and characterized the performance of CNT thin-film transistors. Furthermore, we successfully demonstrated active matrix seven-segment PDLC displays using CNT driver transistors. Our achievements open up opportunities for future nanotube-based, flexible thin-film transparent display electronics.**

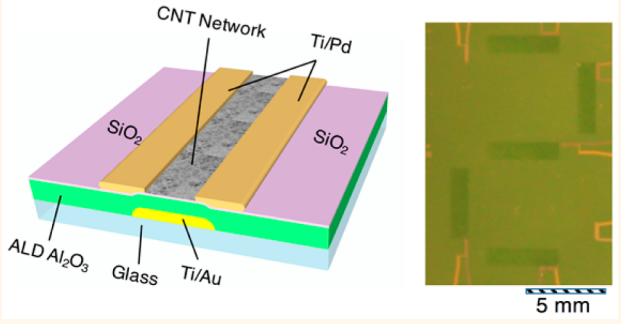

KEYWORDS: *active matrix, transparent display, carbon nanotubes, thin-film transistors, PDLC*

Transparent display is an emerging technology which offers texts and images in front of a background while enabling people to see the scenery in the back of the panel.[1−3] It enhances the observers' view of world and gives people a better life experience. Furthermore, lightweight, energy saving, and other advantages make transparent display a hot area of research.[2,4−7] Polymer-dispersed liquid crystal (PDLC) and organic light-emitting diodes (OLEDs) are the two major candidates for transparent display applications. In particular, with no polarizers, PDLC is the most promising technology due to its simple structure, good chemically stability, and nonemissive property.[2,6,8] Besides, its mechanical flexibility makes flexible transparent display possible. Rigid and flexible PDLC transparent displays have been demonstrated, driven by thin-film transistors (TFTs) with amorphous Si (a-Si)[2,6] and organic thin-film[9−11] channel materials, respectively. However, there are still remaining issues with these transistor channel materials. Amorphous silicon is not intrinsically flexible or transparent. Although organic materials are flexible, they are easy to degrade upon exposure to oxygen and moisture, and thus sophisticated passivation techniques are necessary. In addition, the low mobilities (~1 $cm^2\ V^{-1}\ S^{-1}$) of both a-Si[12] and organic materials[13] are not preferred for large-area display. It is thus desirable to figure out transistor channel materials which are not only intrinsically flexible and transparent but also possess good air stability and high mobility for flexible transparent display applications. Carbon nanotubes (CNTs), as promising channel materials, can meet all the aforementioned requirements.[14] Flexible high-performance CNT integrated circuits have already been demonstrated.[15,16] With the progress in CNT growth,[17−20] purification,[21−23] characterization,[24] and fabrication techniques,[25−29] CNT thin-film transistors (CNT-TFTs) are becoming more and more promising for transparent displays. Active matrix organic light-emitting diodes (AMOLEDs) driven by CNT-TFTs have been reported by various groups including our own.[30−32] On the other hand, PDLC display driven by CNT-TFTs has not been reported yet.

In this paper, we report a monolithically integrated active matrix PDLC seven-segment display with CNT-TFT-based

Received: July 25, 2016
Accepted: October 17, 2016

DOI: 10.1021/acsnano.6b04951
ACS Nano XXXX, XXX, XXX−XXX

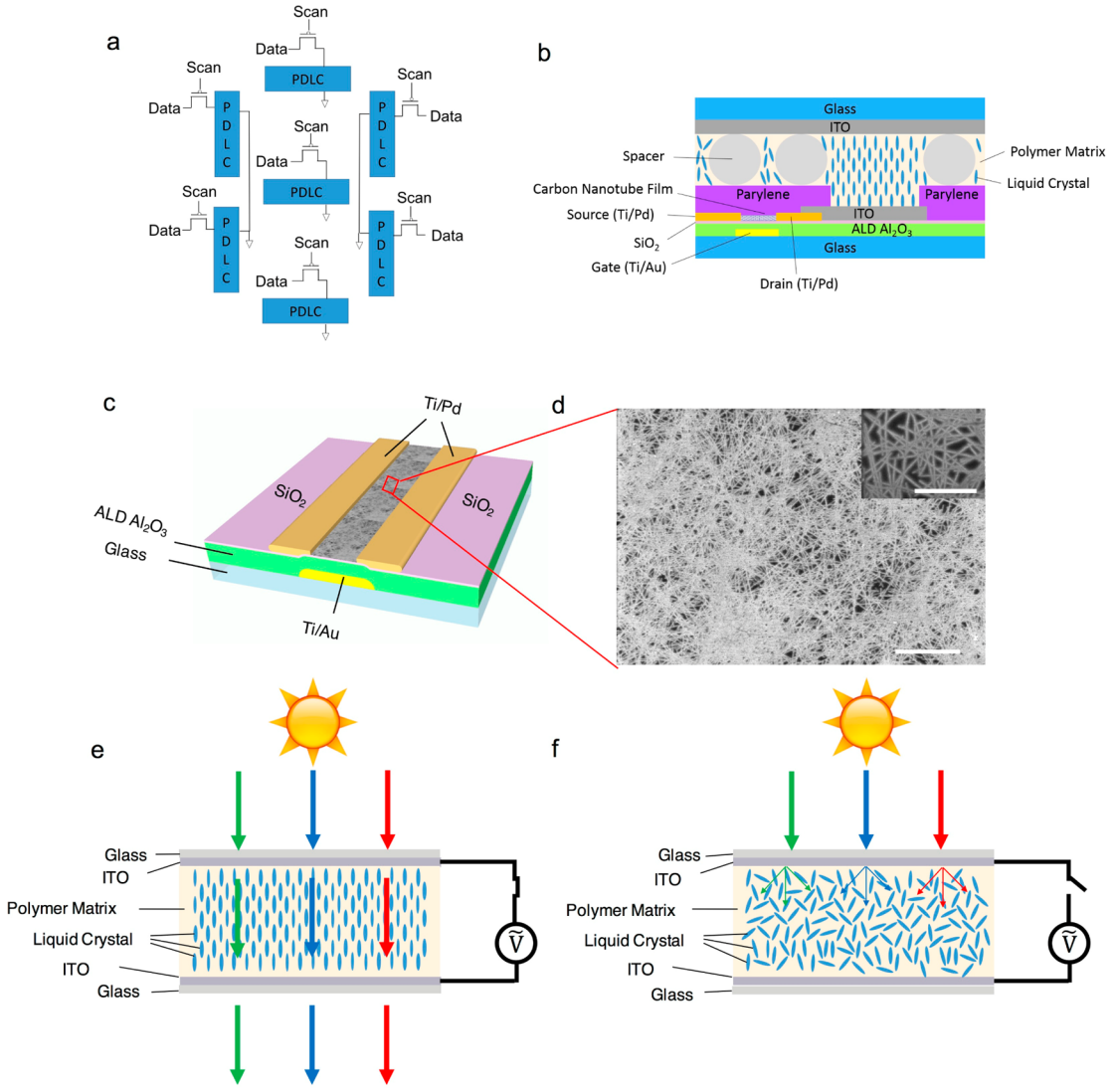

Figure 1. (a) Schematic of the proposed seven-segment CNT-TFT driven PDLC display. (b) The cross-sectional view of the CNT-TFT driven PDLC display, showing the structural details. (c) The side view of the schematic of individual back-gated CNT-TFTs. (d) SEM images of the CNT network. Scale bar is 2 μm. Inset, scale bar is 500 nm. (e) Transparent state and (f) opaque state of the PDLC pixel. When electric field is applied to the electrodes, liquid crystals align with the electric field, permitting the incoming light to pass through in (e). When no electric field is applied, liquid crystals are randomly aligned, and incoming light is scattered, giving opaque state in (f).

control circuits. First, the CNT-TFTs were fabricated using polymer sorted CNTs and show good electrical performance with an average device mobility of 13.23 $cm^2/(V{\cdot}s)$ and on/off ratio of 1.29×10^6. In addition, the PDLC transmission properties were well studied. More importantly, we have successfully monolithically integrated the CNT-TFTs and the PDLC pixels to demonstrate fully functioning seven-segment displays. Our achievements open up great opportunities for future flexible CNT-based thin-film transparent display electronics.

RESULTS AND DISCUSSION

The schematic of a CNT-TFT-driven seven-segment PDLC display is depicted in Figure 1a. Each PDLC display pixel has a CNT driver transistor. In each transistor, the source is connected to the data signal, which is the alternating current (AC) voltage required to drive the PDLC display. The gate of the driver transistor is connected to the scan signal, which turns the PDLC pixel on and off. The structural details of the PDLC display are depicted in a cross-sectional image in Figure 1b. The side view of the schematic of individual back-gated CNT-TFTs is shown in Figure 1c, and the scanning electron microscope (SEM) images show the uniform CNT network in the channel area in Figure 1d. The CNT-TFTs start from a blank glass substrate. The back gate is e-beam evaporated Ti/Au. Atomic layer deposition (ALD) Al_2O_3 acts as the high κ gate dielectric. Another thin layer of SiO_2 on top of Al_2O_3 can improve CNT adhesion, as reported previously.[25,31] The channel material is the high semiconducting ratio random CNT network. Ti/Pd source (S) and drain (D) complete the transistor structure. We notice that a passivation layer of parylene is necessary to avoid performance degradation of the transistor in the integrated structure.[33] For PDLC pixels, the PDLCs are sandwiched between two transparent indium tin oxide (ITO) electrodes. The two electrodes face each other, and their overlapping area defines the active region. To connect the PDLC pixel to the driving transistor, the pixel's bottom ITO electrode overlaps with the drain of the transistor. Depending on the on or off

DOI: 10.1021/acsnano.6b04951
ACS Nano XXXX, XXX, XXX−XXX

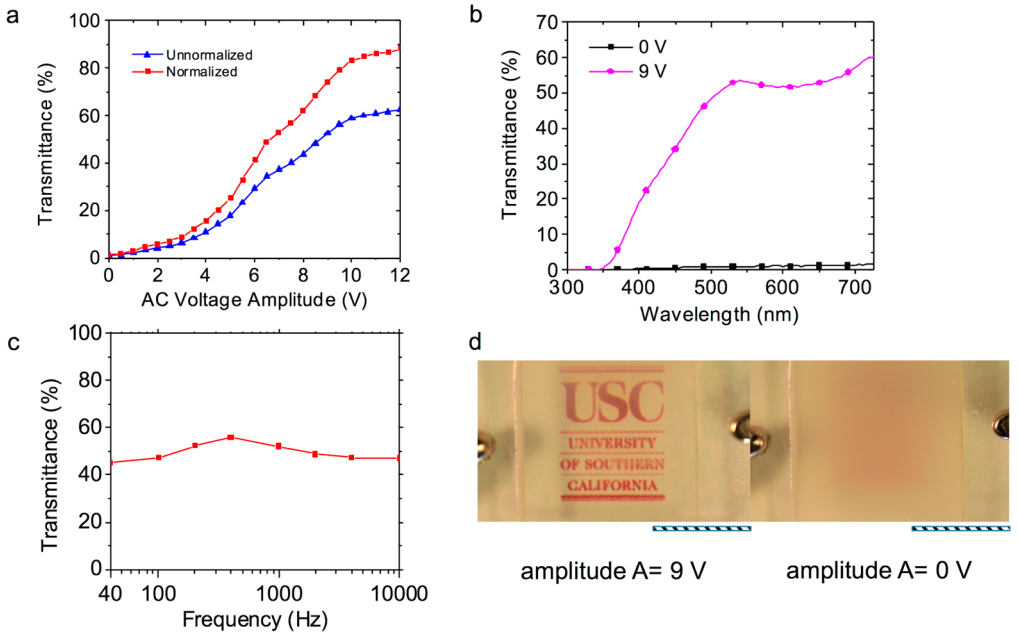

Figure 2. PDLC transmission properties. (a) The raw and normalized transmittance of the PDLC cell at 565 nm wavelength and 400 Hz frequency *versus* AC voltage amplitude. (b) Transmittance of transparent (9 V) and opaque (0 V) states *versus* wavelength. (c) The transmittance of PDLC *versus* AC voltage frequency at 9 V amplitude and 565 nm wavelength (d) Transparent (left) and opaque (right) states in front of printed text. In the transparent state, one can clearly see the printed text through the PDLC cell, while in the opaque state, the text can hardly be seen. Scale bars are 1 cm.

state of the PDLC pixel, the active region allows or blocks the passing through of the incoming light, exhibiting transparent and opaque states, respectively.

PDLCs are composite materials which take advantage of both the solid polymers and fluid liquid crystals. Solid-like PDLC films are formed by embedding microsized liquid crystals into polymer matrices. No polarizers are required for PDLC displays.[34] Instead, when an electric field is applied, the liquid crystal droplets are aligned in the same orientation, where the refractive indices of the liquid crystal droplets and the polymer matrix are the same. The incoming light can pass through PDLC film and the transparent indium tin oxide (ITO) electrodes in a straight line, giving the display a transparent, on state (Figure 1e), and people call it transparent state. On the other hand, when no electric field is applied, the liquid crystal droplets are randomly aligned, and there are significant differences in refractive indices between the liquid crystal droplets and the polymer matrix. The incoming light is randomly scattered, and the display is in an opaque, off state (Figure 1f), and people call it opaque or scattering state. In some situations, even though the transmission for the randomly scattered light is not low enough to make the display totally opaque, people still call it the opaque state to distinguish from the transparent state. Without the need for polarizers, PDLCs enjoy a wide range of advantages, such as reduced weight, high transparency, low power consumption, and good flexibility. For the CNT-TFT driven PDLC concept to work, we need to study and characterize its components individually, *i.e.*, the PDLC transmission properties and the CNT driver transistor behavior. Below, we will study these components in detail.

Norland optical adhesive 65 (NOA65) has been widely used as the fast photocurable prepolymer for PDLC. Here, we choose NOA65 (Norland Co.) and E7 (Merck) as the prepolymer and nematic liquid crystal for our PDLC, respectively. In order to study the transmission properties of PDLC, we fabricated 1.5 cm × 1.5 cm PDLC test cell without the driving transistor. The NOA65 and E7 were mixed in a weight ratio of 3:7 and then injected between two ITO-coated glasses 7 μm apart with the separation defined by transparent spacers (Magsphere Co.). The structure was subsequently cured by UV irradiation (365 nm wavelength) at 6.0 mJ/(cm^2·s) for 18 min. After fabrication, the spectra of PDLC transmittance were measured by UV−vis spectroscopy (Cary 5000, Varian). Figure 2a shows the raw (blue) and normalized (red) transmittance of the PDLC cell *versus* the applied AC voltage amplitude (A) at 565 nm wavelength and 400 Hz frequency. Previous study shows that the on state PDLC transmittance is the highest at this frequency.[35] The raw transmittance data are the transmittance of whole glass-ITO-PDLC-ITO-glass test cell, while the normalized one only accounts for the PDLC transmittance by dividing the raw transmittance by the bare glass-ITO-ITO-glass structure transmittance. As we can see, with zero electric field, the normalized transmittance is 2.0%. With increasing AC amplitudes, the transmittance increases correspondingly and begins to saturate around 9 V. At 9 V, the normalized transmittance is 80%, meaning the contrast ratio is about 40. The performance of our PDLC cell is similar to a previous low operating voltage PDLC study.[2] According to the analysis, we choose A = 9 V as our data voltage in this study. Furthermore, the transmittance curves *versus* wavelength for the transparent state (pink, A = 9 V) and the opaque (black, A = 0 V) are plotted in Figure 2b. The difference in transmittance between the transparent and opaque states are clearly demonstrated in the visible spectrum. We also studied the effect of signal frequency on PDLC transmission. The transmittance of PDLC *versus* AC voltage frequency at A = 9 V and 565 nm wavelength is plotted in Figure 2c. At 400 Hz, the PDLC transmittance is the highest, which also agrees with literature,[35] and we choose this frequency as the AC driving frequency in this paper. Figure

DOI: 10.1021/acsnano.6b04951
ACS Nano XXXX, XXX, XXX−XXX

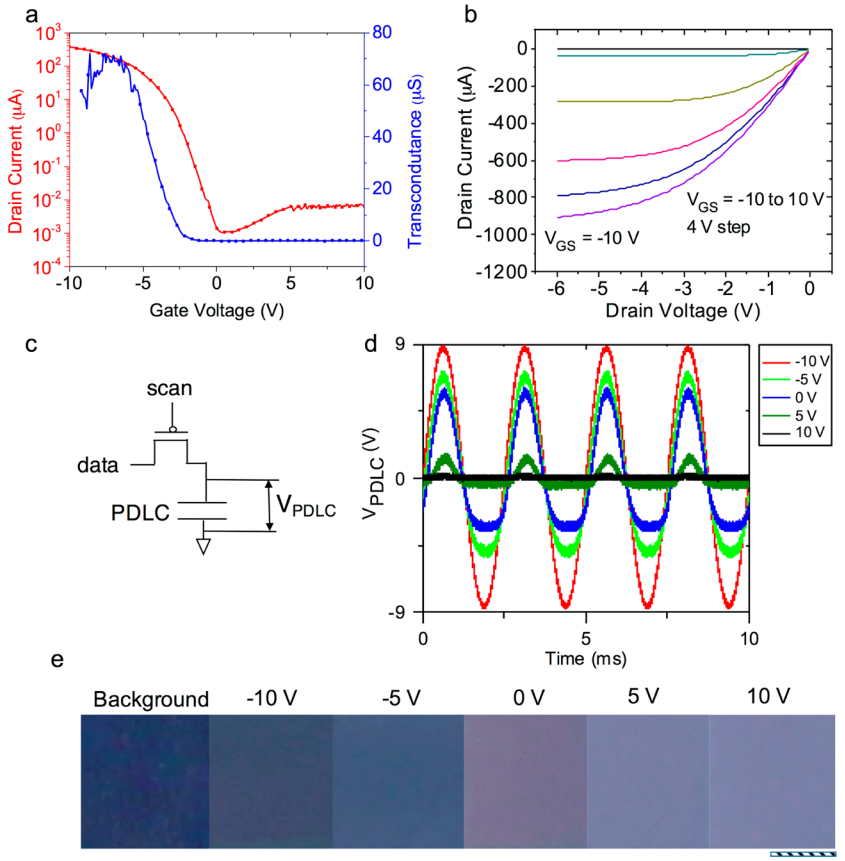

Figure 3. CNT-TFT characteristics and CNT-TFT driven PDLC pixel. (a) Transfer ($I_D - V_G$) characteristics (red) and transconductance $g_m - V_{GS}$ characteristics (blue) of a typical CNT-TFT (L = 20 μm, W = 2400 μm) with V_{DS} = −1 V. (b) Output ($I_{DS} - V_{DS}$) characteristics of the same device with V_G varying from −10 to 10 V in 4 V steps. (c) Schematic of CNT-TFT driven PDLC test cell. The voltage across the PDLC test cell (V_{PDLC}) is indicated. (d) The waveforms of V_{PDLC} under various V_{SCAN} = −10, −5, 0, 5, and 10 V with the data electrode fixed at 400 Hz sine wave, and the amplitude V_{DATA} = 9 V. (e) Optical photographs showing the background blue color without PDLC test cell and the color through PDLC test cell with the driving CNT-TFT under different V_{SCAN}. The CNT-TFT can fully turn on and off the transistor. Scale bar is 1 mm.

2d shows the PDLC test cell with printed text in the background in the transparent (left) and opaque (right) states. As for the transparent state, one can easily see the printed text through the PDLC cell, while for the opaque state, the light is scattered by the PDLC, and the printed text can hardly be seen. The 2.0% transmittance in the opaque state causes slight color variations in the center and the edge of the PDLC cell, and the opaque state transmittance is similar to a previous low operating voltage PDLC study.[2] On the other hand, the high contrast between transparent and opaque states proves that our PDLCs are suitable for CNT-TFT driven PDLC display study.

In order to gain more insight into the final active matrix PDLC display, we fabricated and characterized the electrical performance of the CNT driving transistors. Individual back-gated devices with the same dimensions (L = 20 μm, W = 2400 μm) as in the final structure were fabricated. High semiconducting purity (>99.9% semiconducting single wall CNTs, Nanointegris) CNT network was used as the channel. Detailed fabrication steps are described in the Methods. Note that we used parylene to passivate the transistors, and this passivation layer does not affect the transistor performance significantly (see Figure S1), which agrees with previous studies.[33] This passivation layer is critical, as direct contact of PDLCs with the transistors in the integrated structure can degrade transistor performance. The transfer characteristics ($I_{DS} - V_{GS}$) of a representative CNT-TFT after parylene passivation are presented in the red curve in Figure 3a, and the corresponding transconductance ($g_m - V_{GS}$) is also plotted (blue) in the same graph. The V_{DS} is kept constant at −1 V. This transistor demonstrates a high on/off ratio of 3.09× 10^5, and the mobility extracted using the parallel plate model is 9.59 $cm^2\ V^{-1}\ S^{-1}$. Figure 3b shows the output ($I_{DS} - V_{DS}$) characteristics of the same transistor with V_{GS} varying from −10 to 10 V with 4 V steps. The output curve shows the good saturation behavior and ohmic contacts of the transistor. The analysis shows the good field-effect transistor behaviors of our CNT-TFTs. We also note that CNT-TFTs demonstrate mobility higher than both a-Si and organic transistors.[12,13]

To further understand the behavior of the CNT-TFT controlled PDLC display, we connected the PDLC test cell to the CNT driving transistor externally *via* wire bonding. The active area of the PDLC test cell was modified to 2 mm × 2 mm to match the PDLC pixel area in the final seven-segment display. The schematic of this testing circuit is shown in Figure 3c, and the voltage across the PDLC test cell (V_{PDLC}) is also indicated. From a previous typical direct current (DC) characteristic of the CNT-TFT, we see that the on state resistance of typical driving transistor is around 10 kΩ. Assuming the dielectric constant of the PDLC is 20, the corresponding capacitance is calculated to be ∼0.1 nF. At 400

DOI: 10.1021/acsnano.6b04951
ACS Nano XXXX, XXX, XXX−XXX

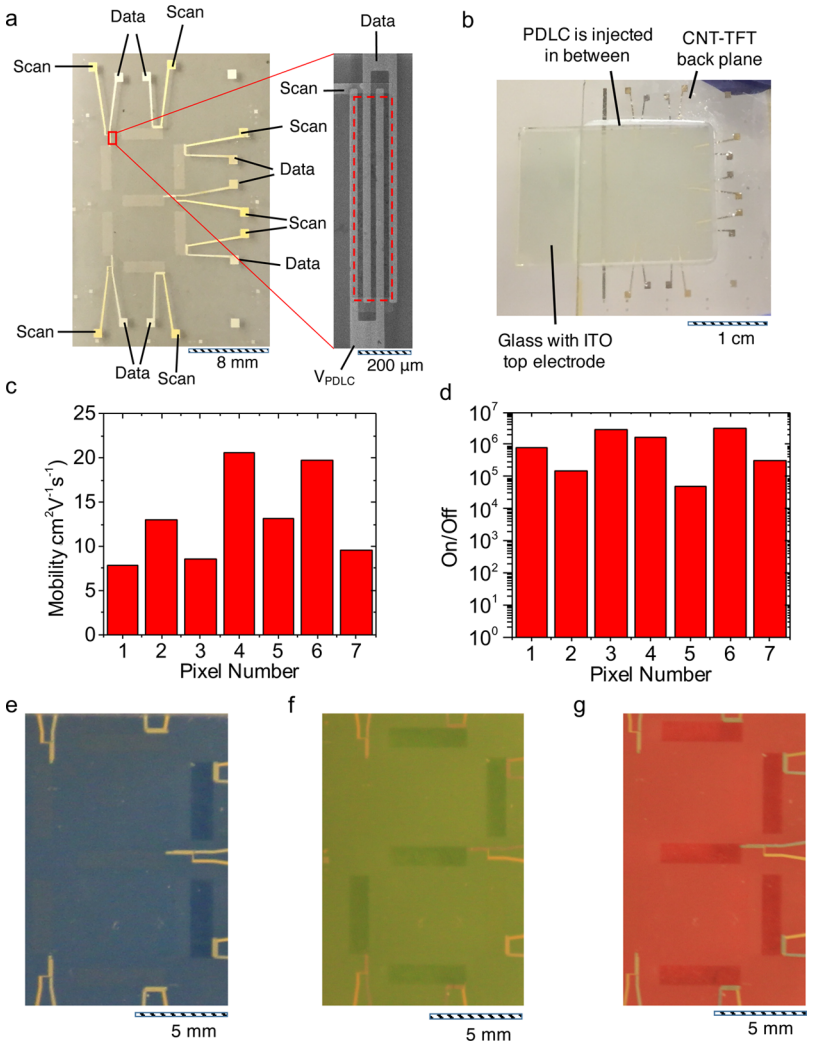

Figure 4. (a) The optical image of the CNT-TFT back panel before integration. The data and scan signals given to each electrode are also indicated. Inset: the SEM image of the CNT-TFT. The dotted region indicates where the CNT film exists. The electrode that will be connected to PDLC pixel with the voltage V_{PDLC} in the later integrated circuit is also shown. (b) The optical image of the seven-segment display after PDLC integration. The CNT-TFT back panel, the glass with ITO top electrode, and the gap where PDLC is injected are also indicated. (c) Histogram of the mobilities of each CNT-TFT driving the seven-segment display. (d) Histogram of the on/off of each CNT-TFT driving the seven-segment display. (e–g) Optical images of the seven-segment display against (e) blue, (f) green, and (g) red backgrounds, displaying digits "1", "2", and "3", respectively.

Hz driving frequency, the impedance of the PDLC is 4.0 MΩ, which is ∼400 times larger than the impedance of the driving transistor, indicating the latter has very little effect on the PDLC performance. On the other hand, the off state impedance of the driving transistor is at least 200 MΩ, which is 50 times larger than the impedance of the PDLC. To confirm our estimations, we measured the waveforms of V_{PDLC} with the data electrode fixed at 400 Hz sine wave with the amplitude V_{DATA} = 9 V. The waveforms of V_{PDLC} under various V_{SCAN} = −10, −5, 0, 5, and 10 V are plotted in Figure 3d. The positive peaks for the corresponding waveforms are 98.3%, 76.0%, 63.1%, 14.7%, and 1.13% of V_{DATA}, respectively, whereas the negative peaks are 96.7%, 54.3%, 35.9% 3.49%, and 0.33% of V_{DATA}, respectively. At V_{SCAN} = 10 V, the maximum peak of V_{PDLC} is 0.10 V, and the pixel remains in the opaque state, while at V_{SCAN} = −10 V, the maximum peak value becomes 8.86 V, and the pixel is in the transparent state. The obvious change in the transmission of the PDLC cell can be visually seen in response with the change in V_{SCAN} against blue background in Figure 3e. The optical photographs represent the blue background without the presence of PDLC test cell as well the PDLC test cell in front of the blue background under various V_{SCAN} voltages of −10, −5, 0, 5, and 10 V, respectively. The contrast demonstrates that the PDLC test cell can be fully turned on and off at V_{SCAN} voltages of −10 and 10 V, and these voltages are chosen as the on and off voltages of the scan lines of the PDLC.

The final accomplishment was to integrate the essential components and demonstrate active matrix seven-segment PDLC display. First, seven-segment back panel CNT-TFT control circuit was fabricated following the same procedures as the individual back-gated devices described previously. A 200 nm radio frequency (RF) sputtered ITO connects to the drain of CNT-TFTs and defines the active pixel area of the PDLC. After depositing parylene passivation layer throughout the whole structure, the parylene above the ITO areas and the probing pads were photolithographically patterned and subsequently removed by oxygen plasma. The PDLC mixture

DOI: 10.1021/acsnano.6b04951
ACS Nano XXXX, XXX, XXX−XXX

was prepared and assembled with the back panel following the same recipe as the PDLC test cell. The optical image of the CNT-TFT back panel before integration is shown in Figure 4a. The inset shows the zoomed-in SEM image of the details of a CNT-TFT. The red dotted region indicates where the CNT film exists. Figure 4b is the optical image of the final structure after integration. The details of the final structure are what we proposed earlier in Figure 1b. The relative positions of the ITO on glass top top electrode, the CNT-TFT back panel, and the gap in between where PDLC was injected are also indicated in Figure 4b. The vertical alignment marker in the left part of the back panel was patterned together with the source and drain of the transistor but does not play any role in the circuit. The top ITO electrode sticks out to the left of the back panel, where it connects to the ground in the circuit. In our back panel, the CNT-TFTs driving the seven-segment PDLC display demonstrate an average mobility of 13.23 $cm^2/(V{\cdot}s)$. The histogram of the mobilities of these seven CNT-TFTs is plotted in Figure 4c. The mobility is similar to a previous publication.[25]

In PDLC display, the current passing through the driving transistor charges and discharges the capacitance of the PDLC pixel, so the on/off ratio is another important transistor parameter. Figure 4d shows the distribution of the on/off ratio of the CNT-TFTs after passivation in the seven-segment display. As we can see, all the transistors demonstrate on/off ratio larger than 5×10^4 with an average of 1.28×10^6, and the champion device has an on/off ratio of 4.3×10^6. The high on/off ratio and the uniformity in device performance guarantee the control circuits can fully turn off the PDLC pixel.

In our PDLC displays, both the scan lines and the data lines are individually controlled for each seven-segment PDLC pixel, so that each pixel can be individually addressed using the CNT-TFTs at different data line voltages (0 to 9 V) with different scan line voltages (−10 to 10 V). Figure 4e–g shows the optical images of the seven-segment PDLC display with numerical digits "1", "2", and "3" against blue, green, and red backgrounds, respectively. While the areas outside of the seven PDLC pixels remain opaque, only the seven pixels can act as the active areas and switch between transparent and opaque states depending on the states of their driving CNT-TFTs. One can observe different background colors through the pixels when they are transparent. The PDLC display can show different and easily recognizable numerical digits against different backgrounds. Our CNT-TFT driven PDLC displays can serve as a starting point for future improvements and developments of flexible and high-performance transparent displays. For example, the rigid substrates and the metal pads can be replaced by bendable materials to enable flexible features. ITO or other transparent conducting materials can be used as the electrodes of the CNT-TFTs to make the structure fully transparent, *etc.* Our work demonstrates the great potential of semiconductor-enriched CNT-TFTs in flexible transparent display applications.

CONCLUSION

The work presents the great potential of using CNT-TFTs for transparent display electronics. We successfully fabricated good contrast PDLC pixels and high-performance CNT-TFTs and achieved their monolithic integration to active matrix, CNT-TFT-driven PDLC displays. The demonstration takes advantage of high mobility, high on/off CNT-TFTs to fully control PDLC pixels in active matrix display. We envision that the transparency and flexibility of the CNTs can add more features to future transparent displays. Our achievements may open a door to future flexible CNT-based transparent displays.

METHODS

Fabrication of Individual Back-Gated CNT-TFTs. The blank glass slide was first cleaned by oxygen plasma at RF power 100 W and O_2 pressure 150 mT for 5 min. The back gates were patterned by photolithography. Five nm Ti and 35 nm Au were sequentially deposited, followed by liftoff. 90 nm of ALD Al_2O_3 and 10 nm e-beam evaporated SiO_2 were deposited onto the whole surface. The sample went through another photolithography to define the exposed area of the bottom gate contact pads. The sample was dipped into 7:1 buffered oxide etch for 90 s to remove the dielectric above the pads. High semiconducting purity (>99.9% semiconducting single wall CNTs, Nanointegris) CNT solution was drop casted onto the sample for 2 min to form a semiconducting CNT network. After incubation, excess CNT solution was washed away by toluene, and the sample was baked at 200° for 1 h. The source and drain electrodes were defined by another round of photolithography, followed by 1 nm Ti/50 nm Pd deposition and subsequent liftoff. Unwanted CNTs outside the channel area were etched away by oxygen plasma at 100 W and 150 mT for 80 s.

ASSOCIATED CONTENT

Supporting Information

The Supporting Information is available free of charge on the ACS Publications website at DOI: 10.1021/acsnano.6b04951.

Details on the parylene passivation effects (S1) is provided (PDF)

AUTHOR INFORMATION

Corresponding Author

*E-mail: chongwuz@usc.edu.

Notes

The authors declare no competing financial interest.

ACKNOWLEDGMENTS

We would like to acknowledge the collaboration of this research with King Abdul-Aziz City for Science and Technology (KACST) *via* The Center of Excellence for Nanotechnologies (CEGN). We also would like to thank Dr. Chien-Yie Tsay from Feng Chia University for useful discussions.

REFERENCES

(1) Gorrn, P.; Sander, M.; Meyer, J.; Kroger, M.; Becker, E.; Johannes, H. H.; Kowalsky, W.; Riedl, T. Towards See-Through Displays: Fully Transparent Thin-Film Transistors Driving Transparent Organic Light-Emitting Diodes. *Adv. Mater.* **2006**, *18*, 738–741.

(2) Su, C. W.; Chen, M. Y. Polymer-Dispersed Liquid Crystal Applied in Active-Matrix Transparent Display. *J. Disp. Technol.* **2014**, *10*, 683–687.

(3) Facchetti, A.; Marks, T. J. *Transparent Electronics: From Synthesis to Applications*; John Wiley and Sons, Ltd: Chichester, U.K., 2010.

(4) Zhang, J. L.; Wang, C.; Zhou, C. W. Rigid/Flexible Transparent Electronics Based on Separated Carbon Nanotube Thin-Film Transistors and Their Application in Display Electronics. *ACS Nano* **2012**, *6*, 7412–7419.

(5) Ju, S.; Li, J. F.; Liu, J.; Chen, P. C.; Ha, Y. G.; Ishikawa, F.; Chang, H.; Zhou, C. W.; Facchetti, A.; Janes, D. B.; Marks, T. J. Transparent Active Matrix Organic Light-Emitting Diode Displays Driven by Nanowire Transistor Circuitry. *Nano Lett.* **2008**, *8*, 997–1004.

DOI: 10.1021/acsnano.6b04951
ACS Nano XXXX, XXX, XXX–XXX

(6) Su, C. W.; Liao, C. C.; Chen, M. Y. Color Transparent Display Using Polymer-Dispersed Liquid Crystal. *J. Disp. Technol.* **2016**, *12*, 31−34.
(7) Lim, T.; Kim, H.; Meyyappan, M.; Ju, S. Photostable Zn_2SnO_4 Nanowire Transistors for Transparent Displays. *ACS Nano* **2012**, *6*, 4912−4920.
(8) Chung, S. H.; Noh, H. Y. Polymer-Dispersed Liquid Crystal Devices with Graphene Electrodes. *Opt. Express* **2015**, *23*, 32149−32157.
(9) Mach, P.; Rodriguez, S. J.; Nortrup, R.; Wiltzius, P.; Rogers, J. A. Monolithically Integrated, Flexible Display of Polymer-Dispersed Liquid Crystal Driven by Rubber-Stamped Organic Thin-Film Transistors. *Appl. Phys. Lett.* **2001**, *78*, 3592−3594.
(10) Sheraw, C. D.; Zhou, L.; Huang, J. R.; Gundlach, D. J.; Jackson, T. N.; Kane, M. G.; Hill, I. G.; Hammond, M. S.; Campi, J.; Greening, B. K.; Francl, J.; West, J. Organic Thin-Film Transistor-Driven Polymer-Dispersed Liquid Crystal Displays on Flexible Polymeric Substrates. *Appl. Phys. Lett.* **2002**, *80*, 1088−1090.
(11) Lee, J.; Kim, D. H.; Kim, J. Y.; Yoo, B.; Chung, J. W.; Park, J. I.; Lee, B. L.; Jung, J. Y.; Park, J. S.; Koo, B.; Im, S.; Kim, J. W.; Song, B.; Jung, M. H.; Jang, J. E.; Jin, Y. W.; Lee, S. Y. Reliable and Uniform Thin-Film Transistor Arrays Based on Inkjet-Printed Polymer Semiconductors for Full Color Reflective Displays. *Adv. Mater.* **2013**, *25*, 5886−5892.
(12) Han, L.; Mandlik, P.; Wagner, S. A New Gate Dielectric for Highly Stable Amorphous-Silicon Thin-Film Transistors With ∼ 1.5 $cm^2/V•s$ Electron Field-Effect Mobility. *IEEE Electron Device Lett.* **2009**, *30*, 502−504.
(13) Kumar, B.; Kaushik, B. K.; Negi, Y. S. Perspectives and Challenges for Organic Thin Film Transistors: Materials, Devices, Processes and Applications. *J. Mater. Sci.: Mater. Electron.* **2014**, *25*, 1−30.
(14) Cao, Q.; Kocabas, C.; Meitl, M. A.; Kang, S. J.; Park, J. U.; Rogers, J. A. Single Walled Carbon Nanotubes for High Performance Thin Film Electronics. In *Carbon Nanotube Electronics*; Javey, A., Kong, J., Eds.; Springer: New York, 2009; pp 211−246.
(15) Sun, D. M.; Timmermans, M. Y.; Tian, Y.; Nasibulin, A. G.; Kauppinen, E. I.; Kishimoto, S.; Mizutani, T.; Ohno, Y. Flexible High-Performance Carbon Nanotube Integrated Circuits. *Nat. Nanotechnol.* **2011**, *6*, 156−161.
(16) Cao, Q.; Kim, H. S.; Pimparkar, N.; Kulkarni, J. P.; Wang, C. J.; Shim, M.; Roy, K.; Alam, M. A.; Rogers, J. A. Medium-Scale Carbon Nanotube Thin-Film Integrated Circuits on Flexible Plastic Substrates. *Nature* **2008**, *454*, 495−500.
(17) Bhaviripudi, S.; Mile, E.; Steiner, S. A.; Zare, A. T.; Dresselhaus, M. S.; Belcher, A. M.; Kong, J. CVD Synthesis of Single-Walled Carbon Nanotubes from Gold Nanoparticle Catalysts. *J. Am. Chem. Soc.* **2007**, *129*, 1516−1517.
(18) Liu, B. L.; Ren, W. C.; Gao, L. B.; Li, S. S.; Pei, S. F.; Liu, C.; Jiang, C. B.; Cheng, H. M. Metal-Catalyst-Free Growth of Single-Walled Carbon Nanotubes. *J. Am. Chem. Soc.* **2009**, *131*, 2082−2083.
(19) Liu, J.; Wang, C.; Tu, X. M.; Liu, B. L.; Chen, L.; Zheng, M.; Zhou, C. W. Chirality-controlled synthesis of single-wall carbon nanotubes using vapour-phase epitaxy. *Nat. Commun.* **2012**, *3*, 1199.
(20) Zhang, F.; Hou, P. X.; Liu, C.; Wang, B. W.; Jiang, H.; Chen, M. L.; Sun, D. M.; Li, J. C.; Cong, H. T.; Kauppinen, E. I.; Cheng, H. M. Growth of Semiconducting Single-Wall Carbon Nanotubes with a Narrow Band-Gap Distribution. *Nat. Commun.* **2016**, *7*, 11160.
(21) Arnold, M. S.; Green, A. A.; Hulvat, J. F.; Stupp, S. I.; Hersam, M. C. Sorting Carbon Nanotubes by Electronic Structure Using Density Differentiation. *Nat. Nanotechnol.* **2006**, *1*, 60−65.
(22) Mistry, K. S.; Larsen, B. A.; Blackburn, J. L. High-Yield Dispersions of Large-Diameter Semiconducting Single-Walled Carbon Nanotubes with Tunable Narrow Chirality Distributions. *ACS Nano* **2013**, *7*, 2231−2239.
(23) Gui, H.; Chen, H. T.; Khripin, C. Y.; Liu, B. L.; Fagan, J. A.; Zhou, C. W.; Zheng, M. A Facile and Low-Cost Length Sorting of Single-Wall Carbon Nanotubes by Precipitation and Applications for Thin-Film Transistors. *Nanoscale* **2016**, *8*, 3467−3473.
(24) Cai, L.; Zhang, S. M.; Miao, J. S.; Wei, Q. Q.; Wang, C. Capacitance-Voltage Characteristics of Thin-film Transistors Fabricated with Solution-Processed Semiconducting Carbon Nanotube Networks. *Nanoscale Res. Lett.* **2015**, *10*, 291.
(25) Chen, H. T.; Cao, Y.; Zhang, J. L.; Zhou, C. W. Large-Scale Complementary Macroelectronics Using Hybrid Integration of Carbon Nanotubes and IGZO Thin-Film Transistors. *Nat. Commun.* **2014**, *5*, 4097.
(26) Brady, G. J.; Joo, Y.; Wu, M. Y.; Shea, M. J.; Gopalan, P.; Arnold, M. S. Polyfluorene-Sorted, Carbon Nanotube Array Field-Effect Transistors with Increased Current Density and High On/Off Ratio. *ACS Nano* **2014**, *8*, 11614−11621.
(27) Zhao, Y. D.; Li, Q. Q.; Xiao, X. Y.; Li, G. H.; Jin, Y. H.; Jiang, K. L.; Wang, J. P.; Fan, S. S. Three-Dimensional Flexible Complementary Metal-Oxide-Semiconductor Logic Circuits Based On Two-Layer Stacks of Single-Walled Carbon Nanotube Networks. *ACS Nano* **2016**, *10*, 2193−2202.
(28) Wei, H.; Shulaker, M.; Wong, H. S. P.; Mitra, S. Monolithic Three-Dimensional Integration of Carbon Nanotube FET Complementary Logic Circuits. In Proceedings from the *IEEE International Electron Devices Meeting (IEDM)*, Washington, DC, December 9−11, 2013; IEEE: New York, 2013.
(29) Liu, X. L.; Han, S.; Zhou, C. W. Novel Nanotube-on-Insulator (NOI) Approach Toward Single-Walled Carbon Nanotube Devices. *Nano Lett.* **2006**, *6*, 34−39.
(30) Wang, C.; Hwang, D.; Yu, Z. B.; Takei, K.; Park, J.; Chen, T.; Ma, B. W.; Javey, A. User-Interactive Electronic Skin for Instantaneous Pressure Visualization. *Nat. Mater.* **2013**, *12*, 899−904.
(31) Zhang, J. L.; Fu, Y.; Wang, C.; Chen, P. C.; Liu, Z. W.; Wei, W.; Wu, C.; Thompson, M. E.; Zhou, C. W. Separated Carbon Nanotube Macroelectronics for Active Matrix Organic Light-Emitting Diode Displays. *Nano Lett.* **2011**, *11*, 4852−4858.
(32) Zou, J. P.; Zhang, K.; Li, J. Q.; Zhao, Y. B.; Wang, Y. L.; Pillai, S. K. R.; Demir, H. V.; Sun, X. W.; Chan-Park, M. B.; Zhang, Q. Carbon Nanotube Driver Circuit for 6 × 6 Organic Light Emitting Diode Display. *Sci. Rep.* **2015**, *5*, 11755.
(33) Selvarasah, S.; Li, X. H.; Busnaina, A.; Dokmeci, M. R. Parylene-C Passivated Carbon Nanotube Flexible Transistors. *Appl. Phys. Lett.* **2010**, *97*, 153120.
(34) Cox, S. J.; Reshetnyak, V. Y.; Sluckin, T. J. Theory of Dielectric and Optical Properties of PDLC films. *Mol. Cryst. Liq. Cryst. Sci. Technol., Sect. A* **1998**, *320*, 301−319.
(35) Yang, K. J.; Kang, J. K.; Choi, B. D. Electro Optic Characteristics of Polymer-Dispersed Liquid-Crystal Films for Flexible Display. *Jpn. J. Appl. Phys.* **2014**, *53*, 08NF03.

DOI: 10.1021/acsnano.6b04951
ACS Nano XXXX, XXX, XXX−XXX